On the relationship between LFP beta oscillation amplitude and firing rate of individual neurons in monkey motor cortex

Joachim Confais[1,#], Nicole Malfait[1], Thomas Brochier[1], Alexa Riehle[1,2], Bjørg Elisabeth Kilavik[1,*]

1 Institut de Neurosciences de la Timone (INT), UMR 7289, CNRS, Aix-Marseille Université, Marseille, France

2 Institute of Neuroscience and Medicine (INM-6), Jülich Research Centre, Jülich, Germany

Present address: Cynbiose, Marcy l'Étoile, France

* Corresponding author: bjorg.kilavik@univ-amu.fr

ABSTRACT

Beta oscillations are prominent in motor cortical local field potentials (LFPs), and their relationship to the local neuronal spiking activity has been extensively studied. Many studies have shown that in motor cortex, spikes of individual neurons tend to lock to the phase of LFP beta oscillations. However, there are contradictory results concerning whether there is also an intrinsic relationship between the amplitude of LFP beta oscillations and the firing rate of individual neurons. To resolve this controversial issue, we correlated the LFP beta oscillation amplitude recorded in macaque motor cortex with spike counts of individual neurons during visuomotor behavior, in two different manners. First, in an analysis termed *task-related correlation*, we included data obtained across all behavioral task epochs. These task-related correlations were frequently significant, and of either negative or positive sign. Second, in an analysis termed *trial-by-trial correlation*, we included only data from a well-defined steady-state pre-cue epoch, and calculated the correlations across trials. Such trial-by-trial correlations were weak and rarely significant. We conclude that there is no intrinsic relationship between the spike count of individual neurons and LFP beta oscillation amplitude in macaque motor cortex, beyond each of these signals being modulated by external factors such as the behavioral task.

INTRODUCTION

The properties of macaque motor cortical local field potential (LFP) beta oscillations have been the focus of many studies. These oscillations occur as short-duration events, so-called beta bursts (Murthy and Fetz 1996; Donoghue et al. 1998; Feingold et al. 2015; Sherman et al. 2016; Lundqvist et al 2016; van Ede et al. 2018), typically lasting between 100-500ms. Beta bursts are not locked to external events (but see Reimer and Hatsopoulos 2010), and vary in their precise moments of occurrence across trials. They are however related to the task (event-related), such that the probability of observing beta bursts changes across task epochs (e.g. Feingold et al. 2015). The individual beta bursts also vary in amplitude, oscillation frequency and duration (Kilavik et al. 2012; Feingold et al. 2015), as well as in their local spatiotemporal dynamics (Rubino et al. 2006; Denker et al. 2018; Rule et al. 2018). Furthermore, several studies addressed the relationship between motor cortical LFP beta oscillations and the local spiking activity (e.g. Murthy and Fetz 1996; Donoghue et al. 1998; Baker et al. 1999; Denker et al. 2011; Canolty et al. 2012; Engelhard et al. 2013; Rule et al. 2017, 2018; Best et al. 2017; Riehle et al. 2018).

Soon after their first description (Berger 1929), human electroencephalographic (EEG) and electrocorticographic (ECoG) sensorimotor beta oscillations were linked to sensorimotor 'idling' (Jasper and Penfield 1949). Furthermore, periods of EEG and magnetoencephalographic (MEG) beta event-related synchronization (ERS) and desynchronization (ERD) were interpreted as reflecting deactivation and activation, respectively, of the sensorimotor cortex (Salenius et al. 1997; Pfurtscheller and Lopes da Silva 1999; Pfurtscheller 2001; Neuper et al. 2006; Bechthold et al. 2018). This concept mainly springs from the robust observations of much reduced beta

oscillation amplitude before movement onset and during movements (Kilavik et al. 2013). The notion that motor cortical beta ERD (ERS) indexes neuronal activation (deactivation) (Neuper et al. 2006) might suggest that one should expect to observe an inverse relationship between neuronal spike rates and beta amplitude. The pioneering studies by Murthy and Fetz (1996) and Donoghue et al. (1998) addressed this issue in the macaque monkey. One study found no difference in the rate of neurons in relation to beta amplitude (Murthy and Fetz, 1996), whereas the other found some locations with increased firing rates during increased oscillation amplitude, and other locations with the opposite (Donoghue et al. 1998). Unfortunately, these partly contradictory results remain overlooked in more recent studies.

Canolty et al. (2012) studied in great detail the relationship between LFP beta oscillations and neuronal spiking in macaque motor cortex. They demonstrated several distinct dependencies between LFP beta amplitude and the firing rates of individual neurons, which they termed 'amplitude-to-rate' mapping. Some neurons exhibited a strong negative correlation and others a strong positive correlation with beta amplitude. Furthermore, the amplitude-to-rate mapping of individual neurons could be reversed across behavioral contexts (manual vs. brain control task). They concluded that the dependency of spike rates upon beta amplitude (internal factor) was conditioned upon the specific behavioral task (external factor). Womelsdorf et al. (2013) followed up by suggesting that by means of this amplitude-to-rate mapping, beta activity could mediate switches between sub-networks across different task epochs, and across tasks. This supposes an intrinsic relationship between beta amplitude and firing rate.

Recently, Rule et al. (2017) also addressed this topic, and found no consistent relationship between LFP beta amplitude and spike rates. Differences in data analysis approaches might be the cause of the different conclusions of these two studies. Canolty et al. (2012) analyzed data by including all task epochs. Rule et al. (2017) restricted their analysis to steady-state movement preparation periods.

To resolve this issue, which remains controversial, we correlated macaque motor cortical LFP beta oscillation amplitude with neuronal spike counts during visuomotor behavior (Kilavik et al. 2012; Confais et al. 2012). When analyzing data acquired during all behavioral task epochs, correlations are frequently observed, confirming the results of Canolty et al. (2012). However, when restricting the analysis to the pre-cue epoch in the same dataset, and performing a trial-by-trial correlation analysis, significant correlations were rare, confirming the results of Rule et al. (2017). We conclude that only a minority of neurons modulate their firing rate in relation to beta amplitude (intrinsic mapping), beyond a simple co-modulation driven by task events.

MATERIALS AND METHODS

We analyzed LFP signals and spiking data recorded simultaneously on multiple electrodes in motor cortex of two macaque monkeys during the performance of a visuomotor delayed center-out reaching task (Kilavik et al. 2010, 2012; Confais et al. 2012). We have already shown that this dataset contains strong LFP oscillations in the beta range, which are systematically modulated in amplitude and peak frequency by the behavioral task (Figure 1; Kilavik et al. 2012). We have also reported on robust and specific modulations in neuronal spiking activity in relation to the behavioral task (Confais et al. 2012).

Animal preparation and data recording

Two adult male Rhesus monkeys (T and M, both 9kg) participated in this study. Care and treatment of the animals during all stages of the experiments conformed to the European and French Government Regulations. In this study we use previously obtained data, from which other results have been presented (Kilavik et al. 2010, 2012, 2014; Ponce-Alvarez et al. 2010; Confais et al. 2012).

After learning an arm-reaching task (see below) the monkeys were prepared for multi-electrode recordings in the right hemisphere of the motor cortex, contra-lateral to the trained arm. The recording chamber locations above motor cortex were verified with T1-weighted MRI scans in both monkeys, and also with intra-cortical micro-stimulation in monkey M (see details in Kilavik et al. 2010). The recordings spanned a region of about 4 and 13mm diameter on the surface in monkeys T and M, respectively (Kilavik et al. 2010).

A multi-electrode, computer-controlled microdrive (MT-EPS, AlphaOmega, Nazareth Illith, Israel) was used to transdurally insert up to four or eight (in monkey T and M, respectively) microelectrodes. The reference was common to all electrodes and positioned, typically together with the ground, on a metal screw on the saline-filled metallic recording chamber. In monkey T the electrodes were organized in a bundle in one common larger guide tube holding the individual electrode guides, with an inter-electrode distance <400µm (MT; AlphaOmega). However, since the electrodes were driven independently, their position in depth varied for each electrode. In monkey M, on some days electrodes were organized in a bundle as for monkey T and on others the electrodes were positioned independently within the chamber with separate guide tubes (Flex-MT; AlphaOmega), thus resulting in up to 13mm inter-electrode distance. The amplified raw signal (1 Hz – 10 kHz) was digitized and stored at 32 kHz. For the online extraction of single neuron activity, the amplified raw signal was high-pass filtered at 300Hz to obtain the high-frequency signal, on which an online spike shape detection method was applied (MSD, AlphaOmega, Nazareth Illith, Israel), allowing isolation of up to three single neurons per electrode. The timing of each spike was then stored as TTLs at a temporal resolution of 32 kHz, down-sampled offline to 1 kHz before analysis. Offline spike sorting on the raw signals was additionally performed in Matlab (The MathWorks Inc., USA) by using Principal Component Analysis in the toolbox MClust (http://www.stat.washington.edu/mclust/) when the online spike sorting was considered as non-optimal. In parallel, the amplified raw signal was low-pass filtered online at 250Hz to obtain the low-frequency LFP signal, which was stored with a temporal resolution of 1 kHz. Behavioral

data were transmitted online to AlphaMap (AlphaOmega) from the CORTEX software (NIMH, http://dally.nimh.nih.gov), which was used to control the task.

Behavioral task

We trained the two monkeys to make arm-reaching movements in 6 directions in the horizontal plane from a common center position, by holding a handle that was freely movable in the two-dimensional plane (Figure 1A). In some sessions, only 2 random-chosen opposite directions were used to reduce the session duration, concerning 21% and 39% of the analyzed sessions in monkey T and M, respectively. The monkeys had continuous monitor feedback about hand (white cursor) and the 6 possible target positions (red outlines).

Two delays were presented successively in each trial. During the first delay (D1) the monkey had to wait for the visual spatial cue (SC; see below), which was briefly presented following a cued interval duration. The second delay (D2) entailed visuomotor integration and movement preparation while waiting for the GO signal. Delay duration (short or long) was modulated from trial to trial in a pseudo-random fashion, but was kept the same for both delays within one trial. The monkey started each trial by moving the handle to the center ('start' in Figure 1A) and holding it there for 700ms until a temporal cue (TC) was presented. TC consisted of a 200ms long tone, its pitch indicating the delay duration, starting at the end of the tone (low pitch for short and high pitch for long delay duration). The short and long delay durations were fixed to 700 and 1500ms for monkey T, 1000 and 2000ms for monkey M. The delay that followed TC (D1) involved temporal attention processes (Confais et al. 2012), to perceive SC that was illuminated very briefly (55ms) at the end of the delay at one of the peripheral target position. To assure the temporal precision of SC

illumination time and duration, light-emitting diodes (LEDs) were used, which were mounted in front of the computer screen in fixed positions at the center of the 6 peripheral red target outlines, on a transparent plate. SC was subsequently masked by the additional illumination of the 5 remaining LEDs, marking the start of D2. During D2 the movement direction indicated by the visual cue SC had to be memorized and prepared. All LEDs went off at the end of D2 (GO signal), indicating to the monkey to reach towards and hold (for 300ms) the correct peripheral target position. The reaction and movement times were computed online to reward the monkey after target hold, with a maximum allowance of 500ms for each. For data analysis, the reaction times were redefined offline using the arm trajectories. Trajectories were measured in x and y vectors at 1ms resolution. The mean of each x and y vector during the 500ms before GO in each trial was used as the movement's starting position. The moment when reaching a 2mm deviation, minus a fixed latency of 35ms (average movement duration from the starting position to the threshold), was determined as movement onset. From each of the two vectors (x and y), the shortest time was defined as RT. These values were controlled by visual inspection of single trial trajectories (see Kilavik et al. 2010).

--- Figure 1 near here ---

Data selection and analysis

While the monkeys performed the reaching task we recorded neuronal activity from motor cortex. We recorded 90 sessions in 37 days in monkey T and 151 sessions in 73 days in monkey M. Consecutive sessions in the same day were made after lowering further the electrodes to sample new neurons. This

provided a total of 287 and 759 individual recording sites in monkeys T and M, respectively. A site is here defined as the conjunction of a specific chamber coordinate of the electrode entry and the cortical depth. After site elimination due to lack of sufficiently recorded trials, or large recording artifacts affecting either the lower (LFP) or higher (spiking activity) frequencies, 127 and 358 sites remained for further analysis, from 66 and 135 individual sessions, for monkeys T and M, respectively. These essentially constitute the conjunction between the LFP datasets studied in Kilavik et al. (2012) and the single neuron datasets studied in Confais et al. (2012).

All analyses were conducted offline by using Matlab (The MathWorks, Inc.). We studied a low beta band that was strong in both animals. In addition, in monkey M who also had a marked beta band at higher frequency (see Kilavik et al. 2012), we repeated the analysis for this band. We first band-pass filtered the LFP around the average peak beta frequency for each band with a zero-phase 4^{th} order Butterworth filter. In monkey T we filtered between 22+/-5Hz to capture the dominant low beta band across the entire trial (see example in Figure 1F and averages across all LFPs in Kilavik et al. 2012). For monkey M, to capture the low and high beta bands across the entire trial we filtered the LFP at 19+/-5Hz and 32+/-5Hz, respectively (see Figure 1G and Kilavik et al. 2012). After filtering, beta oscillation amplitude was estimated from the analytical filtered LFP, as the envelope of the signal from the Hilbert transform.

From the online and offline spike sorting, typically 1 to 3 neurons were available on each electrode. For the correlation analyses between LFP beta amplitude and neuronal firing rate, beta-neuron pairs were constructed using signals from different simultaneously recorded sites. This choice was guided by findings demonstrating the possibility of spike contamination of LFP signals

recorded on the same electrode, also for the lower LFP frequency ranges studied here (Zanos et al. 2011; Waldert et al. 2013). From the 127 and 358 acceptable sites, 320 and 671 beta-neuron pairs were constructed in monkeys T and M, respectively.

In these pairs, some trials with obvious artifacts (mainly due to teeth grinding or static electricity) detected by visual inspection, were excluded from further analysis (less than 5% of all trials). After trial elimination, and considering the variable duration for which the monkeys were willing to work in different behavioral sessions, the analyzed beta-neuron pairs contained at least 10 correct trials in each movement direction, although typically 20 or more correct trials were available per direction. The average numbers of correct trials in each direction (in short or long delay trials) across pairs were 23+/-5SD for monkey T and 20+/-5SD for monkey M. The average numbers of total short (long) delay trials for each pair were 117+/-36SD (117+/-37SD) for monkey T and 93+/-36SD (90+/-36SD) for monkey M.

Task-related correlations between LFP beta amplitude and neuronal spike counts

We here define *task-related correlation* as the correlation between two brain signals calculated across several diverse task epochs, such that the concurrent modulations in the brain signals related to the unfolding task events and related behavior can be expected to influence the amount of correlation observed between them. The task-related correlation was calculated between LFP beta oscillation amplitude and neuronal spike counts for each beta-neuron pair. Data recorded in all epochs between the trial start (initial central touch) and until 1000ms after the GO signal was included (complete trial as shown in

Figure 2A-B), analyzed separately for short and long delay trials. Across the included session, the average reaction times were 161 (206) ms in monkey T and 232 (255) ms in monkey M, in short (long) delay trials, and the average movement times were 303 (296) ms in monkey T and 297 (303) ms in monkey M, in short (long) delay trials (see also Kilavik et al. 2010). Thus, average reaction and movement times were both shorter than their maximally allowed durations of 500ms each, so that the analysis typically also includes most of the required 300ms target-hold time. Note that the average reaction times were significantly shorter in short delay trials, probably due to the improved temporal anticipation of the GO cue in short than in long delay trials (discussed in Kilavik et al. 2010).

The beta-neuron correlations were calculated separately for the preferred and non-preferred (opposite) movement direction for the neuron in each pair, where preferred direction was taken as the one with maximal trial-averaged spike rate any time after the presentation of SC up to trial end. We decided to analyze both the preferred and the non-preferred direction for each neuron, since one can envisage that the task-related correlation with the LFP beta oscillations might depend on the type of involvement of the neuron in coding for the cued movement.

The single trial data in these two directions was cut in 300ms non-overlapping consecutive windows. The window duration of 300ms was partly chosen based on the typical duration of beta bursts in our dataset (200-500ms), see example in Figure 2B; see also Murthy and Fetz 1992). Note that recent literature suggests that in some contexts beta bursts can be of much shorter duration than seen in our dataset (e.g. Feingold et al. 2015; Sherman et al. 2016; Lundqvist et al 2016). Since our 300ms windows were aligned to the task

timing, i.e. signal occurrences, and beta bursts do not have a fixed temporal relationship with such external events (see introduction), some windows will overlap with a beta burst, while others will fall in a period with low beta amplitude, and some will partly overlap with a beta burst.

We furthermore considered 300ms to be a minimal duration needed to have meaningful (non-zero) spike counts in a majority of individual windows. In addition, we restricted our analysis to the subsets of beta-neuron pairs for which the average firing rate of the neuron, across all 300ms windows, was above 3 Hz. The number of analyzed pairs thus varied slightly for short and long delay trials and for preferred and non-preferred movement directions, as detailed in Table 1 (see also Figure 1B-E).

This trial cutting provided 11 (16) non-overlapping 300ms windows in monkey T and 13 (19) in monkey M, for short (long) delay trials. The total number of windows accumulated across trials varied because of variable number of correctly performed trials across sessions. The average numbers of overall available windows for all trials in the same (preferred or non-preferred) movement direction were 259+/-64SD (373+/-96SD) for monkey T and 283+/-77SD (400+/-113SD) for monkey M, in short (long) delay trials. The average beta amplitude (Hilbert envelope; see Figure 2B) and the spike counts in each 300ms window (providing one value per signal type in each window) was then used to calculate the beta-neuron task-related correlation (see example in Figure 2C), quantified with the Spearman's rank order correlation (Spearman's rho). Correlations with $p<0.01$ were considered significant, but the complete distributions of rho values across the populations of beta-neuron pairs are always presented, to allow appreciating the magnitude of the different types of correlations.

The analysis approach just described resembles as closely as possible for our dataset the approach used by Canolty et al. (2012). They concatenated LFP and spike data across several recording sessions from implanted multi-electrode arrays, providing between 58-410 minutes of continuous data, including all task epochs. However, in our dataset, there were on average more than twice as many windows available for this task-related correlation analysis approach compared to the number of trials (averages of 117 in both short and long for monkey T and 93 and 90 in short and long, respectively, for monkey M; see above) available for the trial-by-trial correlation analysis that we describe in the next section. This difference may pose problems in comparing the results due to sample size affecting the statistical power. To permit a more direct comparison between the task-related correlation analysis and the trial-by-trial correlation, we therefore repeated the analysis after selecting from the total available windows a subset equaling the number of short (or long) delay trials for each beta-neuron pair. As far as possible, this selection was done such that every second window was excluded. The selection of every second window was repeated if there were still too many windows. Finally this selection was complemented with additional (previously excluded) windows if needed, to arrive at the correct number of windows. The correlation using this window selection procedure is shown for the example pair in Figure 2C, and the results across all datasets are detailed in Table 1.

Trial-by-trial correlations between LFP beta amplitude and neuronal spike counts

The *trial-by-trial correlation* between LFP beta oscillation amplitude and neuronal spike counts for each beta-neuron pair was calculated in a 300ms

epoch immediately preceding SC, across all trials, separately for short and long delay trials (gray epoch in Figure 2A-B). Since our 300ms window was aligned to SC, and beta bursts do not have a fixed temporal relationship with the external events (see introduction, and example in Fig. 2B), on some trials the window overlaps with a beta burst, while in some trials it will fall in a period with lower beta amplitude, and in some trials it will partly overlap in time with a beta burst. These different degrees of overlap will also occur for the task-related correlation, as described above.

As for the task-related correlation analysis, we restricted our analysis to the subsets of beta-neuron pairs for which the average firing rate of the neuron in the pre-SC epoch was above 3 Hz. We choose this restricted task moment by considering it to be the epoch in which the monkey's behavioral state was most likely to be similar across all trials within each delay duration condition. Specifically, the monkey maintained a stable arm position on the central target and was awaiting the presentation of a visual cue. Notably, this epoch started between 1.3-2.6 seconds after the monkey had moved his hand cursor into the central target to start a new trial, and 0.4-1.7 seconds after the end of the presentation of the auditory temporal cue (TC off) providing information about delay duration. In this epoch the movement direction was still unknown, so that we can group all directions in the analysis, while analyzing short and long delay trials separately. Significant trial-by-trial beta-neuron correlations in this epoch may be mainly related to modulations of internal (anticipatory) processes, thereby reflecting any intrinsic beta-spike relationship, independent of external factors related to the task such as the processing of external visual or auditory sensory cues or overt movements. This analysis is more closely comparable to the analysis performed by Rule et al. (2017), in which they

restricted their analysis to delays considered to entail steady-state movement preparation. However they compared epochs inside and outside of beta bursts, thus at varying moments in their 1 second duration delays considered. As we already described for the current dataset, the neuronal spike rates modulated significantly from the start to the end of the delay (D1) preceding SC, some neurons systematically increasing and others decreasing their rate between TC and SC (Confais et al. 2012). Thus, in our case, this delay cannot be considered as steady-state in its entirety. To avoid these systematic, task-related modulations in neuronal firing rates influencing our analysis, we restricted our window to the final 300ms prior to the pre-indicated moment of SC onset.

We filtered the LFP to capture the main beta frequency band(s) for each animal as described above. We used the average beta amplitude (Hilbert envelope) and the spike counts in each trial in this 300ms epoch for analysis (providing one value per signal type per trial window). The trial-by-trial correlation for each beta-neuron pair was then quantified as the Spearman's rank order correlation (see example in Figure 2D), as described above for the task-related correlation analysis.

--- Figure 2 near here ---

Phase-locking of neuronal spiking to LFP beta phase

We wanted to confirm that the LFP beta oscillations were at least partially of local origin, by verifying that a substantial proportion of the neurons significant locked their spiking activity to the LFP beta phase. We quantified the proportion of neurons with a significant phase-locking to beta oscillations in a 300ms duration pre-SC epoch, separately for short and long delay trials. We

chose to focus on this particular task epoch since one of the analyses of correlations between beta-amplitude and neuronal spike counts was done on this same epoch (the trial-by-trial correlation). We only included neurons with at least 50 spikes in this 300ms epoch, accumulated across all trials, to ensure a reliable statistical analysis. This restricted our analysis to a subset of 229 (226) of the 320 pairs in monkey T and 441 (448) of the 671 pairs in monkey M, for short (long) delay trials. Beta phase was extracted from the Hilbert transformation of the beta-filtered LFP, and the phase at each spike time was determined.

To quantify the phase locking, we first used Rayleigh's test of non-uniformity of circular data (CircStat Matlab toolbox; Berens 2009). To determine whether the locking was significant for individual neurons, we used a trial-shuffling method. Beta oscillations are typically not phase-reset by external events (but see Reimer and Hatsopoulos 2010), and the analyzed pre-SC epoch was sufficiently long after the previous external event (0.4-1.7s after TC off), such that any phase-resetting effects should have minimal effect in this epoch. This makes trial-shuffling an efficient method for obtaining a 'baseline' measure of phase locking, destroying the temporal relationship between the two signals, while preserving their individual properties such as rhythmicity.

We ran 1000 repetitions of the phase-locking analysis (Rayleigh's test; in the same 300ms pre-SC epoch) while randomly combining beta phases and spike times from different trials. If the original analysis yielded a larger z-statistic value from the Rayleigh's test than 990/1000 (equivalent to $p<0.01$) of the trial-shuffled analyses, we considered the phase-locking of the neuron to be significant.

RESULTS

The aim of this study was to determine to which degree there is an intrinsic relationship between the amplitude of LFP beta oscillations and firing rates (spike counts) of individual neurons in the motor cortex. We correlated motor cortical LFP beta amplitude and neuronal spike counts measured in short windows either along the trial including several different task epochs (*task-related correlation*) or within a fixed task epoch, but across trials (*trial-by-trial correlation*). We start with a general description of the average task-related modulation in firing rate of the included neurons, as well as the typical task-related modulations of LFP beta amplitude.

Task-related modulations in neuronal firing rates and LFP beta amplitude

Figure 1B-E shows the average firing rates of all neurons included in this study, separated for neuronal preferred and non-preferred movement direction. At the population level there was a phasic increase in rate for both the preferred and non-preferred directions following the spatial cue (SC). The population rate then decreased during the preparatory delay between SC and GO, but remained above the pre-SC level in particular for the preferred direction, before increasing again towards and during movement execution after GO. Note that the average rates are somewhat higher already at the start of the trial for the non-preferred direction. This is caused by imposing an average minimal rate of 3Hz. Since the rate is per definition lower after SC for the non-preferred compared to the preferred direction, the somewhat fewer neurons included for the non-preferred direction have slightly higher rate at the start of the trial than the excluded neurons, shifting up the averages.

Example LFP spectrograms for each monkey are shown in Figure 1F-G. These examples are representative when it comes to the average beta power and frequency across task epochs in these datasets, as we already described in detail in Kilavik et al. (2012). Notably monkey T had one dominant beta band, which varied in average frequency between 19-25Hz across task epochs. Monkey M had two dominant beta bands, a low band modulating between 17-21Hz and a high band modulating between 29-34Hz (Kilavik et al. 2012). For both monkeys and both bands, beta power decreased after SC and during movement execution after GO. Note that even if these trial-averaged spectrograms suggest a prolonged increase in beta amplitude during the delays, as can be seen in the example LFP in Figure 2B in reality beta occurs in individual bursts of different duration, amplitude and exact timing across trials (see also Feingold et al. 2015; Sherman et al. 2016; Lundqvist et al 2016).

Task-related correlations between LFP beta amplitude and neuronal spike counts are prominent

We calculated task-related correlations between LFP beta oscillation amplitude and neuronal spike counts along the trial including different task epochs for the 320 and 671 beta-neuron pairs in monkeys T and M, respectively. An example pair with significant task-related correlation is shown in Figure 2C. This particular pair showed a negative correlation between beta amplitude and neuronal firing rate. The overall percentages of significant correlations, for both monkeys and bands, in short and long delay trials and in the neuronal preferred and non-preferred movement directions are summarized in Table 1.

Task-related correlations were prominent and frequently significant for both monkeys, and for both beta bands in monkey M. The complete distributions of Spearman's rho values were rather broad and significantly shifted towards negative values (Wilcoxon signed rank test on Fisher's z-transformed rho values; $p<<0.01$; distributions not shown).

The task-related correlations for the preferred direction were statistically significant ($p<0.01$) in 41-50% of pairs (across both monkeys and bands, short and long delay trials; Table 1). A combination of negative and positive significant correlations was observed, as also described by Canolty et al. (2012). However, the large majority of the significant correlations for neuronal preferred directions were negative (75 to 85% across both monkeys and bands, short and long delay trials). This dominance of negative correlations is possibly due to the systematic decreases in beta amplitude following the visual spatial cue (SC) and during movement execution (see Figure 1F-G; Kilavik et al. 2012, 2013), which occurs more or less concurrently with phasic increases in firing rates in a majority of neurons in their preferred direction (see Figure 1B-E and Confais et al. 2012).

For the neuronal non-preferred movement direction, 36-43% of pairs had significant task-related correlations, across both monkeys and bands, short and long delay trials. However, the proportions of these significant correlations being negative were smaller than for the preferred direction (48-63% across both monkeys and bands, short and long delay trials). After a brief phasic increase in rate following the spatial cue, which at the population level is similar in preferred and non-preferred movement directions (see Figure 1), the neurons discharge less in the non-preferred compared to the preferred movement direction (per definition), and some neurons discharge less than

their pre-cue rate. This could be expected to lead to larger proportions of neurons having a positive correlation with beta amplitude for their non-preferred direction, as beta amplitude also drops after the cue and during movement execution. The proportions of significant negative and positive correlations were very similar for short and long delay trials (Table 1), as would be expected if the movement directional preferences of the neurons were the major cause for the sign of the beta-neuron task-related correlations.

When comparing pairs with significant correlations in both the preferred and the non-preferred directions, of the pairs significant in both directions, only a small fraction changed correlation sign, mainly from negative in preferred to positive in non-preferred (e.g. in short delay trials 4/44 in monkey T, 2/95 and 4/108 in monkey M low and high bands; only 1 pair changed correlation sign from positive to negative, for monkey M low beta band). Thus, the different proportions of significant negative correlations for preferred vs. non-preferred directions mainly stem from those pairs being significantly correlated in only one of the directions. The changes in the sign of task-related correlations between preferred and non-preferred movement directions at the population level can therefore not be interpreted as a 'beta-to-rate remapping' for individual neurons, in the way described by Canolty et al. (2012) when switching between their manual and brain control tasks.

In order to have comparable statistical power as for the trial-by-trial correlation analysis, for which the results will be described in the next section, we also performed the task-related correlation analysis by selecting only as many windows as there were available trials for the trial-by-trial correlation analysis for each individual pair. These are therefore also the results we show in Figures 3-4. This sub-selection of windows reduced the overall proportions of

pairs with significant task-related correlations (15-31% for neuronal preferred movement direction, across both monkeys and bands, short and long delay trials), which is not surprising since we reduce statistical power by reducing the sample sizes. However, the main results of broad distributions of rho values (Figure 3), and a majority of significant correlations being negative (80-88% across both monkeys and bands, short and long delay trials; Table 1) for the preferred direction remained similar. All the distributions of Spearman's rho values were significantly shifted towards negative values (Wilcoxon signed rank test on Fisher's z-transformed rho values; $p<<0.01$; Figure 3). The distributions of rho values remained broad also for the non-preferred direction (Figure 4), but as for the previous analysis, the proportions of the significant correlations (12-25% across both monkeys and bands, short and long delay trials) being negative decreased compared to the preferred direction (49-62% across both monkeys and bands, short and long delay trials; Table 1). Furthermore, the distributions were only significantly shifted away from zero for monkey M (Wilcoxon signed rank test on Fisher's z-transformed rho values; $p<0.01$ for monkey M, $p>0.2$ for monkey T; Figure 4).

For both these analysis approaches, there was a gradual decrease in the proportions of pairs with significant task-related correlations going from preferred direction in short delay trials to non-preferred direction in long delay trials (see Table 1). This might be due to slower or more gradual modulations across task epochs of both beta burst probability and spike counts for longer delays, as these modulations are scaled to delay duration (discussed in Kilavik et al. 2014), in addition to some neurons having shallower modulations in spike counts for their non-preferred direction (Figure 1B-E).

In general these results are in agreement with the conclusions made by Canolty et al. (2012) of many neurons in motor cortex being subject to a 'beta-to-rate mapping', in which there is a specific relationship between the firing rates of individual neurons and the amplitude of beta oscillations.

--- Figures 3 and 4 near here ---

Trial-by-trial correlations between LFP beta amplitude and neuronal spike counts are rare

Figure 2D shows that in the selected example beta-neuron pair, LFP beta amplitude and neuronal spike count did not correlate trial-by-trial in the pre-SC epoch. This was indeed representative of the populations. Only 3.4-5.6% of the pairs had a significant correlation (across both monkeys and bands, short and long delay trials), with similar proportions of negative and positive correlations (see Table 1). Figure 5 shows the distributions of Spearman's rho values for the pre-SC trial-by-trial correlation analysis in short and long delay trials for the three datasets. The distributions were narrower than for the task-related correlations, and only significantly shifted away from zero center for the low beta band in Monkey M in short delay trials ($p<0.01$, slight shift towards positive rho values, all other $p>0.2$).

The very weak and rarely significant trial-by-trial correlations are in line with the results in Rule et al. (2017), where they describe inconsistent differences in firing rates for low and high beta amplitude events in their steady-state preparatory period analysis.

--- Figure 5 near here ---

Neurons lock their spikes to LFP beta oscillation phase

The LFP is prone to containing a combination of signals generated by local and distant sources (e.g. Kajikawa and Schroeder 2011). When wanting to study the relationship between the LFP beta oscillation amplitude and local spiking activity it is essential to verify the likewise local origin of the beta oscillations. A significant phase-locking of the spiking activity of the local neuronal population reveal locking of the neurons to synchronized synaptic inputs (of local or distant origin), in turn leading to local postsynaptic currents that contribute to generating the LFP (Pesaran et al. 2018). As a control analysis, we therefore confirmed that the spiking activity of a significant proportion of the neurons locked to the phase of the LFP beta oscillations. We specifically performed this control in the pre-SC epoch, where we found only very few neurons with a trial-by-trial spike count modulation in relation to beta amplitude, as described in the previous section.

Overall, in the analyzed pre-SC epoch, 37.6% and 40.7% of the neurons locked significantly their spiking activity to the beta phase of the LFP in monkey T in short and long delay trials, respectively. 11.1% and 12.2% of the neurons locked significantly to the low and high beta bands, respectively, in monkey M in short delay trials, and 8.0% and 14.3% were phase-locked to the low and high band in long delay trials. Interestingly, in monkey M, only 2.0% in short delay trials and 2.7% in long delay trials of the neurons locked significantly their spikes to both the low and the high bands in this task epoch, such that overall 21.3% in short delay trials and 19.6% in long delay trials of the neurons locked their spikes to either the low, high or both LFP beta bands in this monkey. The clear phase-locking found for many neurons in this dataset made us conclude

that the observed LFP beta bands were at least partly locally generated, justifying the subsequent correlation analyses between beta amplitude and neuronal firing rate. Finally, there was no systematic difference in locking prevalence of the few neurons with, compared to without, a significant trial-by-trial correlation of spike count with beta amplitude in the same task epoch.

DISCUSSION

In order to reconcile two apparently contradictory results about the relationship between beta amplitude and neuronal firing rate, we here performed systematic quantifications of correlations between macaque motor cortical LFP beta amplitude and spike counts in individual neurons during a visuomotor task, in two different manners. First, in the analysis called *task-related correlation*, analogous to the approach by Canolty et al. (2012), we included data obtained across all behavioral task epochs. Such task-related correlations were frequent. Second, in the analysis called *trial-by-trial correlation*, analogous to the approach by Rule et al. (2017), we included data only from the pre-cue steady-state epoch, and calculated the trial-by-trial correlation of beta amplitude and spike counts. We found such trial-by-trial correlations to be very rare. We conclude that there is no intrinsic dependency between neuronal spike count and beta amplitude, beyond both types of signals being modulated by external factors such as the behavioral task.

Is there an intrinsic relationship between motor cortical beta oscillation amplitude and the activation level of individual neurons?

The question of whether modulations in beta amplitude are related to modulations in the activation level of local neurons was already examined more than 20 years ago. In a behavioral context in which macaques made reaching movements to a Klüver board, Murthy and Fetz (1996) found no difference in average firing rates of individual neurons inside and outside beta bursts (20-40Hz) in motor cortex. However, they found a decrease in the variability of firing rates of individual neurons during and just after burst events, compared to just before bursts. They also noted that many neurons

were phase-locked to the high-amplitude beta oscillations, which might be the main source of this decreased firing rate variability. Donoghue et al. (1998) analyzed LFPs and neuronal discharge (sorted individual neurons and multi-units) during different tasks involving finger or arm movements. They found one group of multi-units to 'overlap' with LFP oscillations (20-60Hz), increasing their discharge in epochs of increased oscillation amplitude. Another, 'mixed' group mainly decreased their discharge during increased beta oscillation amplitude, but also showed some overlap. The authors noted that the consistency in patterns for each recorded site suggested that these two signals (LFP oscillation amplitude and neuronal discharge rate) might be mechanistically linked.

These two rather contradictory early studies (Murthy and Fetz 1996; Donoghue et al. 1998) cannot be directly compared, since their methods have significant differences (using the spiking activity of single or multi units; considering different LFP frequency ranges, either only high beta or a combination of beta and low gamma; differences in behavioral tasks). Furthermore, they were not cited by subsequent literature addressing the same question. More recently, Canolty and colleagues (2012) presented a rigorous analysis of the 'cross-level coupling' between spikes and beta oscillations, and described an 'amplitude-to-rate mapping'. Some neurons exhibited a strong negative correlation and others a strong positive correlation with beta amplitude, and this mapping could change across tasks (manual or brain control tasks; Canolty et al. 2012). The notion of an amplitude-to-rate mapping supposes an intrinsic relationship between beta amplitude and firing rate, and Womelsdorf et al. (2013) commented that beta activity could index

switches between sub-networks across different task epochs, and different tasks.

Rule et al. (2017) also addressed the same question, and found no consistent relationship between beta amplitude and spike rates when restricting their analysis to steady-state preparation periods. However, they did not confront their results with the Canolty et al. (2012) study, in addition to neither of the two referring to the two studies conducted 20 years ago. Noteworthy, Engelhard et al. (2013) trained macaques to increase motor cortical 30-40Hz LFP oscillation power and spike synchrony, and found no systematic modulation in neuronal firing rates when comparing low and high power periods.

A direct comparison of the two recent studies (Canolty et al. 2012; Rule et al. 2017) suggests that their discrepant conclusions might be due to the different analysis approaches, either including data from all trial epochs, or restricting their analysis to steady-state preparatory periods, respectively. The two ways in which we analyze the data in this study, quantifying both *task-related* and *trial-by-trial* correlations in the same dataset, resemble the approaches used by Canolty et al. (2012) and Rule et al. (2017), respectively. Indeed, we confirm the results of Canolty et al. (2012) when including many different task epochs, comprising the movement phase, and we confirm the results of Rule et al. (2017) when we restrict our analysis to the steady-state pre-cue epoch, analyzed across trials. Rule et al. (2017) compared firing rates inside and outside of beta bursts across a one second delay period, whereas we used a fixed pre-SC window that was not always aligned to the beta bursts. Still we arrive at the same conclusion.

The importance of movement onset in determining beta-neuron 'task-related' correlations was recently demonstrated by Khanna and Carmena (2017), who only analyzed beta amplitude and neuronal firing rates in the epoch surrounding movement onset, confirming and extending the findings of Canolty et al. (2012). Our results therefore reconcile the disparate results from these recent papers, and possibly also the results obtained by Murthy and Fetz (1996) and Donoghue et al. (1998).

Do several processes underlie amplitude modulations of motor cortical beta oscillations?

Rule et al. (2017) pointed to the fact that beta amplitude decreases at movement onset, roughly when neurons in motor cortex are generally mostly active (see also Khanna and Carmena 2017; Best et al. 2017). This observation was in contradiction to their finding of a lacking systematic relationship between beta amplitude and firing rates in their main analysis restricted to the preparatory delay. They therefore proposed that there are two different processes underlying beta amplitude modulations. One is responsible for the beta amplitude decrease around movement onset, and is linked to large modulations in spiking rates, and decreased spiking rhythmicity. Another process underlies the transient beta amplitude modulations (bursts) during steady-state preparatory delays lacking overt movements, which seems decoupled from modulations in spiking activity (rate and rhythmicity).

However, in addition to decreasing around the time of movement onset, motor cortical LFP beta oscillation amplitude also decreases transiently after the presentation of cues informing about parameters of the upcoming movement (Kilavik et al. 2012, 2013; see Figure 1F-G), a phenomenon also

observed in human EEG (e.g. Zaepffel et al. 2013). In the same task period, many motor cortical neurons modulate strongly their discharge, in a cue-selective manner (Confais et al. 2012; Figure 1). These concurrent systematic modulations will surely lead to task-related correlations between beta amplitude and spike counts around cue presentation. However, neither overt movements, nor changes in electromyography (EMG) activity occur at this moment in the task (Kilavik et al. 2010). Thus, in the framework proposed by Rule et al. (2017), a third process would then be responsible for the modulations of beta oscillations in relation to informative cues, different from both the process underlying the transient bursts observable in steady states, decoupled from spiking and EMG modulations, and the process underlying the decrease in beta amplitude at movement onset, accompanied by large modulations in spiking activity and EMG.

Instead, we propose that there is no intrinsic relationship between LFP beta amplitude and neuronal firing rates. Rather, the significant task-related correlations we observe, as well as the beta-to-rate mapping described in Canolty et al. (2012) is simply a reflection of the beta amplitude (burst probability) and firing rates (spiking probability) both being modulated by the task events, however independently from each other. The different proportions of negative and positive task-related correlations for the preferred and non-preferred movement direction of the neurons support this claim.

This implies that there is no need for different processes responsible, respectively, for the modulations of beta bursts in steady state situations and for the suppression of beta bursts during movement execution (and after informative cues), as suggested by Rule et al. (2017). Even if the underlying mechanism might remain the same, this does not exclude potentially different

functional roles for beta oscillation bursts occurring during cue anticipation, during movement preparation or during the movement itself (Kilavik et al. 2013).

Interestingly, the results are very similar for both beta bands in monkey M. Thus no clear distinction can be made concerning potential functional roles of each band in this study, beyond the conclusion that there is no intrinsic relationship between oscillation amplitude and spike counts of individual neurons for any of the two bands.

Phase-locking of spikes to LFP beta oscillations

The lack of an intrinsic relationship between LFP beta amplitude and neuronal activation level (rate) does not exclude other relationships between beta oscillations and neuronal spiking activity. Indeed, as we demonstrate in this dataset, confirming several previous studies (Murthy and Fetz 1996; Donoghue et al. 1998; Baker et al. 1999; Denker et al. 2011; Canolty et al. 2012; Engelhard et al. 2013; Riehle et al. 2018) there is significant locking of spike times to LFP beta oscillation phase in many neurons in motor cortex. Such phase locking may result in rhythmic synchronization among populations of neurons thereby increasing their concerted impact on post-synaptic targets without necessary increasing their spike rates (Destexhe and Paré 1999; Azouz and Gray 2000; Rudolph and Destexhe 2003).

Bridging between intra-cortical signals and EEG/MEG

There are at least three conceptual pitfalls related to the degree large-scale observations of sensorimotor beta amplitude modulations in EEG or MEG can be interpreted in relation to intra-cortical mechanisms. First, EEG/MEG

signals are traditionally analyzed using trial-averaging methods, in which significant beta ERS periods may last up to seconds. However, individual beta episodes or bursts in single trials last only for a fraction of this duration (Pfurtscheller et al. 1996; Murthy and Fetz 1996; Donoghue et al. 1998; Feingold et al. 2015; Shin et al. 2017), and one should therefore be careful not to interpret an ERS seen in trial-averaged data as an extended period of a stable synchronized state.

Second, Best et al. (2017) addressed the spatial smoothing inherent to EEG/MEG, which is reduced for well-referenced intracortical LFPs. Using multi-electrode array recordings, they showed that the movement-related beta ERD can occur with slight differences in timing across only a few millimeters of cortical tissue, a spatial scale too fine to be resolved with EEG/MEG.

The results of the current study are relevant for a third conceptual pitfall. Periods of beta ERS (ERD) were interpreted as reflecting a deactivation (activation) of the sensorimotor cortex (e.g. Pfurtscheller and Lopes da Silva 1999; Neuper et al. 2006), in particular when considering the transition epoch around movement onset (Khanna and Carmena 2017). Several EEG/MEG studies have reported that similar ERS/ERD patterns as those occurring in overt movement tasks can be found in covert tasks involving motor imagery or motor observation/mirroring (e.g. Schnitzler et al. 1997; Hari et al. 1998; Babiloni et al. 2002; Caetano et al. 2007; Kilner et al. 2009; Avanzini et al. 2012; Brinkman et al. 2014). These similarities could be taken as evidence that the underlying neuronal mechanisms are similar for overt and covert motor tasks. However, the general absence of significant trial-by-trial correlations between beta amplitude and neuronal spike counts suggests absence of any intrinsic relationship between them. Then, if the task-related correlation between beta

amplitude and neuronal spike counts merely reflects their concurrent, but nevertheless independent, relationship with the task and the associated behavior, one cannot readily extrapolate to other tasks lacking this specific behavioral component.

ACKNOWLEDGEMENTS

Funding: This work was supported by the Agence National de la Recherche [grant number ANR-NEUR-05-045-1]; Ministère de l'enseignement supérieur et de la recherche (to J.C.). The authors wish to thank Adrian Ponce-Alvarez for participating in animal training and data recording; Ivan Balansard and Marc Martin for animal care; and Joel Baurberg, Alain De Moya, and Xavier Degiovanni for technical assistance.

REFERENCES

Avanzini P, Fabbri-Destro M, Dalla Volta R, Daprati E, Rizzolatti G, Cantalupo G (2012) The dynamics of sensorimotor cortical oscillations during the observation of hand movements: an EEG study. PLoS One 7:e37534.

Azouz R, Gray CM (2000) Dynamic spike threshold reveals a mechanism for synaptic coincidence detection in cortical neurons in vivo. Proc Natl Acad Sci U S A 97:8110–8115.

Babiloni C, Babiloni F, Carducci F, Cincotti F, Cocozza G, Del Percio C, Moretti DV, Rossini PM (2002) Human cortical electroencephalography (EEG) rhythms during the observation of simple aimless movement: a high-resolution EEG study. Neuroimage 17:559–572.

Baker SN, Kilner JM, Pinches EM, Lemon RN (1999) The role of synchrony and oscillation in the motor output. Exp Brain Res 128:109–117.

Bechtold L, Ghio M, Lange J, Bellebaum C (2018) Event-related desynchronization of mu and beta oscillations during the processing of novel tool names. Brain Lang 177–178:44-55

Berens P (2009) CircStat: A Matlab Toolbox for Circular Statistics. J Stat Soft 31:1-21

Berger H (1929) Über das elektrenkephalogramm des menschen. Eur Arch Psychiatry Clin Neurosci 87:527–570.

Best MD, Suminski AJ, Takahashi K, Brown KA, Hatsopoulos NG (2017) Spatio-Temporal Patterning in Primary Motor Cortex at Movement Onset. Cereb Cortex 27:1491-1500.

Brinkman L, Stolk A, Dijkerman HC, de Lange FP, Toni I (2014) Distinct roles for alpha- and beta-band oscillations during mental simulation of goal-directed actions. J Neurosci 34:14783-14792.

Caetano G, Jousmaki V, Hari R (2007) Actor's and observer's primary motor cortices stabilize similarly after seen or heard motor actions. Proc Natl Acad Sci U S A 104:9058-9062

Canolty RT, Ganguly K, Carmena JM (2012) Task-dependent changes in cross-level coupling between single neurons and oscillatory activity in multiscale networks. PLoS Comput Biol 8:e1002809.

Confais J, Kilavik BE, Ponce-Alvarez A, Riehle A (2012) On the anticipatory precue activity in motor cortex. J Neurosci 32:15359–15368.

Denker M, Roux S, Lindén H, Diesmann M, Riehle A, Grün S (2011) The local field potential reflects surplus spike synchrony. Cereb Cortex 21:2681–2695.

Destexhe A, Paré D (1999) Impact of network activity on the integrative properties of neocortical pyramidal neurons in vivo. J Neurophysiol 81:1531–1547.

Donoghue JP, Sanes JN, Hatsopoulos NG, Gaál G 1(998) Neural discharge and local field potential oscillations in primate motor cortex during voluntary movements. J Neurophysiol 79:159--173.

Engelhard B, Ozeri N, Israel Z, Bergman H, Vaadia E (2013) Inducing γ oscillations and precise spike synchrony by operant conditioning via brain-machine interface. Neuron 77:361-375.

Feingold J, Gibson DJ, DePasquale B, Graybiel AM (2015) Bursts of beta oscillation differentiate postperformance activity in the striatum and motor cortex of monkeys performing movement tasks. Proc Natl Acad Sci U S A 112:13687-13692.

Hari R, Forss N, Avikainen S, Kirveskari E, Salenius S, Rizzolatti G (1998) Activation of human primary motor cortex during action observation: a neuromagnetic study. Proc Natl Acad Sci U S A 95:15061-15065.

Jasper H, Penfield W (1949) Electrocorticograms in man: effect of voluntary movement upon the electrical activity of the precentral gyrus. Arch Psychiatr Zeitschr Neurol 83:163-174.

Kajikawa Y, Schroeder CE (2011) How local is the local field potential? Neuron 72:847-858.

Khanna P, Carmena JM (2017) Beta band oscillations in motor cortex reflect neural population signals that delay movement onset. Elife 6:e24573.

Kilavik BE, Confais J, Ponce-Alvarez A, Diesmann M, Riehle A (2010) Evoked potentials in motor cortical LFPs reflect task timing and behavioral performance. J Neurophysiol 104:2338-2351.

Kilavik BE, Confais J, Riehle A (2014) Signs of timing in motor cortex during movement preparation and cue anticipation. Adv Exp Med Biol. 829:121-142

Kilavik BE, Ponce-Alvarez A, Trachel R, Confais J, Takerkart S, Riehle A (2012) Context-related frequency modulations of macaque motor cortical LFP beta oscillations. Cereb Cortex 22:2148-2259.

Kilavik BE, Zaepffel M, Brovelli A, MacKay WA, Riehle A (2013) The ups and downs of beta oscillations in sensorimotor cortex. Exp Neurol 245:15-26.

Kilner JM, Marchant JL, Frith CD (2009) Relationship between activity in human primary motor cortex during action observation and the mirror neuron system. PLoS One 4:e4925.

Lundqvist M, Rose J, Herman P, Brincat SL, Buschman TJ, Miller EK (2016) Gamma and Beta Bursts Underlie Working Memory. Neuron 90:152-164.

Murthy VN, Fetz EE (1996) Synchronization of neurons during local field potential oscillations in sensorimotor cortex of awake monkeys. J Neurophysiol 76:3968-3982.

Neuper C, Wörtz M, Pfurtscheller G (2006) ERD/ERS patterns reflecting sensorimotor activation and deactivation. Prog Brain Res 159:211-222.

Pesaran B, Vinck M, Einevoll GT, Sirota A, Fries P, Siegel M, Truccolo W, Schroeder CE, Srinivasan R (2018) Investigating large-scale brain dynamics using field potential recordings: analysis and interpretation. Nat Neurosci 21:903-919.

Pfurtscheller G, Lopes da Silva FH (1999) Event-related EEG/MEG synchronization and desynchronization: basic principles. Clin Neurophysiol 110:1842-1857.

Pfurtscheller G, Stančák Jr, A, Neuper C (1996) Post-movement beta synchronization. A correlate of an idling motor area? Electroencephalogr Clin Neurophysiol 98:281–293.

Pfurtscheller G (2001) Functional brain imaging based on ERD/ERS. Vis Res 41: 1257-1260

Ponce-Alvarez A, Kilavik BE, Riehle A. (2010) Comparison of local measures of spike time irregularity and relating variability to firing rate in motor cortical neurons. J Comput Neurosci, 29:351-365.

Reimer J, Hatsopoulos NG (2010) Periodicity and evoked responses in motor cortex. J Neurosci 30: 11506-11515

Riehle A, Brochier T, Nawrot M, Grün S (2018) Behavioral context determines network state and variability dynamics in monkey motor cortex. Frontiers Neural Circuits 12:52

Rubino D, Robbins KA, Hatsopoulos NG (2006) Propagating waves mediate information transfer in the motor cortex. Nat Neurosci 9:1549–1557.

Rudolph M, Destexhe A (2003) Tuning neocortical pyramidal neurons between integrators and coincidence detectors. J Comput Neurosci 14: 239-251

Rule ME, Vargas-Irwin CE, Donoghue JP, Truccolo W (2017) Dissociation between sustained single-neuron spiking and transient β-LFP oscillations in primate motor cortex. J Neurophysiol 117:1524-1543.

Rule ME, Vargas-Irwin C, Donoghue JP, Truccolo W (2018) Phase reorganization leads to transient β-LFP spatial wave patterns in motor cortex during steady-state movement preparation. J Neurophysiol 119:2212-2228.

Salenius S, Schnitzler A, Salmelin R, Jousmaki V, Hari R (1997) Modulation of human cortical rolandic rhythms during natural sensorimotor tasks. Neuroimage 5:221-228.

Schnitzler A, Salenius S, Salmelin R, Jousmäki V, Hari R (1997) Involvement of primary motor cortex in motor imagery: a neuromagnetic study. Neuroimage 6:201-208.

Sherman MA, Lee S, Law R, Haegens S, Thorn CA, Hämäläinen MS, Moore CI, Jones SR (2016) Neural mechanisms of transient neocortical beta rhythms: Converging evidence from humans, computational modeling, monkeys, and mice. Proc Natl Acad Sci U S A 113:E4885-94.

Shin H, Law R, Tsutsui S, Moore CI, Jones SR (2017) The rate of transient beta frequency events predicts behavior across tasks and species. Elife 6: e29086.

Torrecillos F, Alayrangues J, Kilavik BE, Malfait N (2015) Distinct Modulations in Sensorimotor Postmovement and Foreperiod β-Band Activities Related to

Error Salience Processing and Sensorimotor Adaptation. J Neurosci 35:12753-12765.

van Ede F, Quinn AJ, Woolrich MW, Nobre AC (2018) Neural Oscillations: Sustained Rhythms or Transient Burst-Events? Trends Neurosci 41:415-417

Waldert S, Lemon RN, Kraskov A (2013) Influence of spiking activity on cortical local field potentials. J Physiol 591:5291-5303.

Womelsdorf T, Westendorff S, Ardid S (2013) Subnetwork selection in deep cortical layers is mediated by beta-oscillation dependent firing. Front Syst Neurosci 7:25.

Zaepffel M, Trachel R, Kilavik BE, Brochier T (2013) Modulations of EEG beta power during planning and execution of grasping movements. PLoS One 8(3):e60060

Zanos TP, Mineault PJ, Pack CC (2011) Removal of spurious correlations between spikes and local field potentials. J Neurophysiol 105:474-486.

FIGURE LEGENDS

Figure 1: Behavioral paradigm, average neuronal rates and example LFP spectrograms

A: Behavioral paradigm. Left, drawing of the experimental apparatus showing the SC epoch (note the cursor on the central fixation dot). Right, Sequence of task events, not to scale. Start indicates the moment when the monkey brings the cursor to the center of the screen to initiate a new trial. The musical note indicates the presentation of a tone. Tone pitch differs according to delay duration. All screen-shots shown in the diagram stay on until the next one appears (cursor is not shown). TC, 200 ms; SC, 55 ms; D1, delay 1, D2, delay 2. Both delays have either short duration (700ms in monkey T and 1000ms in monkey M) or long duration (1500ms in monkey T and 2000ms in monkey M). There is also a 700ms delay between start and TC.

B-E: Average rate for all neurons included in the task-related correlation analysis, for preferred (dark gray) and non-preferred (light gray) movement directions, in short (top) and long (bottom) delay trials for monkey T (left) and monkey M (right). The curves reflect the mean firing rate +/-SEM. The average rate for each SUA was smoothed with a Gaussian filter of length 50ms and sigma 20ms, before averaging.

F-G: Spectrograms of one representative example LFP for each monkey, including all correct long delay trials (session and LFP number marked inside plots). Frequency is on the vertical axis and time along the horizontal axis. Warmer colors indicate increased power (a.u.). After high-pass filtering the LFP at 2Hz with a 4^{th} order Butterworth filter, the spectral power was calculated with the pwelch function in Matlab, based on Welch's method, which windows

the data with a hamming window. We used frequency intervals of 0.1 Hz (i.e., high-density spectrum, implemented by zero-padding the data), and the data in each 300-ms sliding window were analyzed as one section (i.e., not using the default mode of the pwelch function that splits the data in multiple partly overlapping sections). The averages across all long delay trials were plotted at the center of each sliding window.

Figure 2: Example LFP beta - neuron pair from monkey T

A: Raster plot and peri-stimulus time histogram (PSTH) of one example neuron in its preferred movement direction, in short delay trials. In the raster plot, each dot is an action potential and each row a trial, ordered according to reaction times (open circles; shortest on top). The thick black line represents the neuronal activity averaged across all the shown trials (PSTH; smoothed with a Gaussian filter of length 100ms and sigma 50ms). The epoch marked in gray preceding SC (also in B) was used for trial-by-trial correlation analysis shown in D (that also included all short delay trials for all the other movement directions). N in the plots reflects the number of included neurons. Note the slightly reduced numbers for the non-preferred direction, caused by imposing an average minimal rate of 3Hz for each direction separately (see methods).

B: LFP from another co-recorded electrode, filtered for the beta range (22+/-5Hz; light gray curves), shown for the same individual trials as the raster plot for the neuron in A. Darker gray curves show the instantaneous beta oscillation amplitude, was estimated from the analytical filtered LFP, as the envelope of the signal from the Hilbert transform. The thick black line indicates the average

beta amplitude across all the shown trials (smoothed with a Gaussian filter of length 100ms and sigma 50ms).

C: This pair's task-related correlation, for short delay trials in the preferred direction. We show the analysis made by selecting only as many windows as number of trials (n=135). Each dot corresponds to one 300ms window, with combined values of beta amplitude and spike counts. The Spearman's rho was -0.40, a highly significant negative correlation.

D: This pair's trial-by-trial correlation, for short delay trials (n=135). Each dot corresponds to the beta amplitude and spike counts for one trial, in the 300ms pre-cue window marked in gray in A-B. The correlation was not significant.

Figure 3: Task-related correlations in neuronal preferred direction

Complete distributions of Spearman's rho values in neuronal preferred direction, for all pairs in gray and overlaid in black for the significant pairs ($p<0.01$), for short (top row) and long (bottom row) delay trials, for monkey T (left) and monkey M low beta band (LO; middle) and high beta band (HI; right). Dotted lines to the left of the solid lines at zero mark the median of each complete distribution, which was significantly shifted to the left (negative correlations) for all datasets (Wilcoxon signed rank test on Fisher's z-transformed rho values; $p<<0.01$ for all datasets).

Figure 4: Task-related correlations in neuronal non-preferred direction

Complete distributions of Spearman's rho values in neuronal non-preferred direction, for all pairs in gray and overlaid in black for the significant pairs ($p<0.01$), for short (top row) and long (bottom row) delay trials, for monkey T (left) and monkey M low beta band (LO; middle) and high beta band (HI; right). Dotted lines to the left of the solid lines at zero mark the median of each complete distribution, which was weakly but significantly shifted to the left for monkey M (Wilcoxon signed rank test on Fisher's z-transformed rho values; $p<0.01$), but not for monkey T ($p>0.2$).

Figure 5: Trial-by-trial correlations

Complete distributions of Spearman's rho values for all pairs in gray and overlaid in black for the significant pairs ($p<0.01$), for short (top row) and long (bottom row) delay trials, for monkey T (left) and monkey M low beta band (LO; middle) and high beta band (HI; right). Dotted lines mark the median of each complete distribution, which was significantly shifted to the right (positive correlations) only for monkey M, for the low band in short delay trials (Wilcoxon signed rank test on Fisher's z-transformed rho values; $p<0.001$; all others $p>0.2$).

Table 1: Summary of statistics

Number and percent of pairs with significant task-related and trial-by-trial correlations, for monkey T, and monkey M low (LO) and high (HI) beta bands.

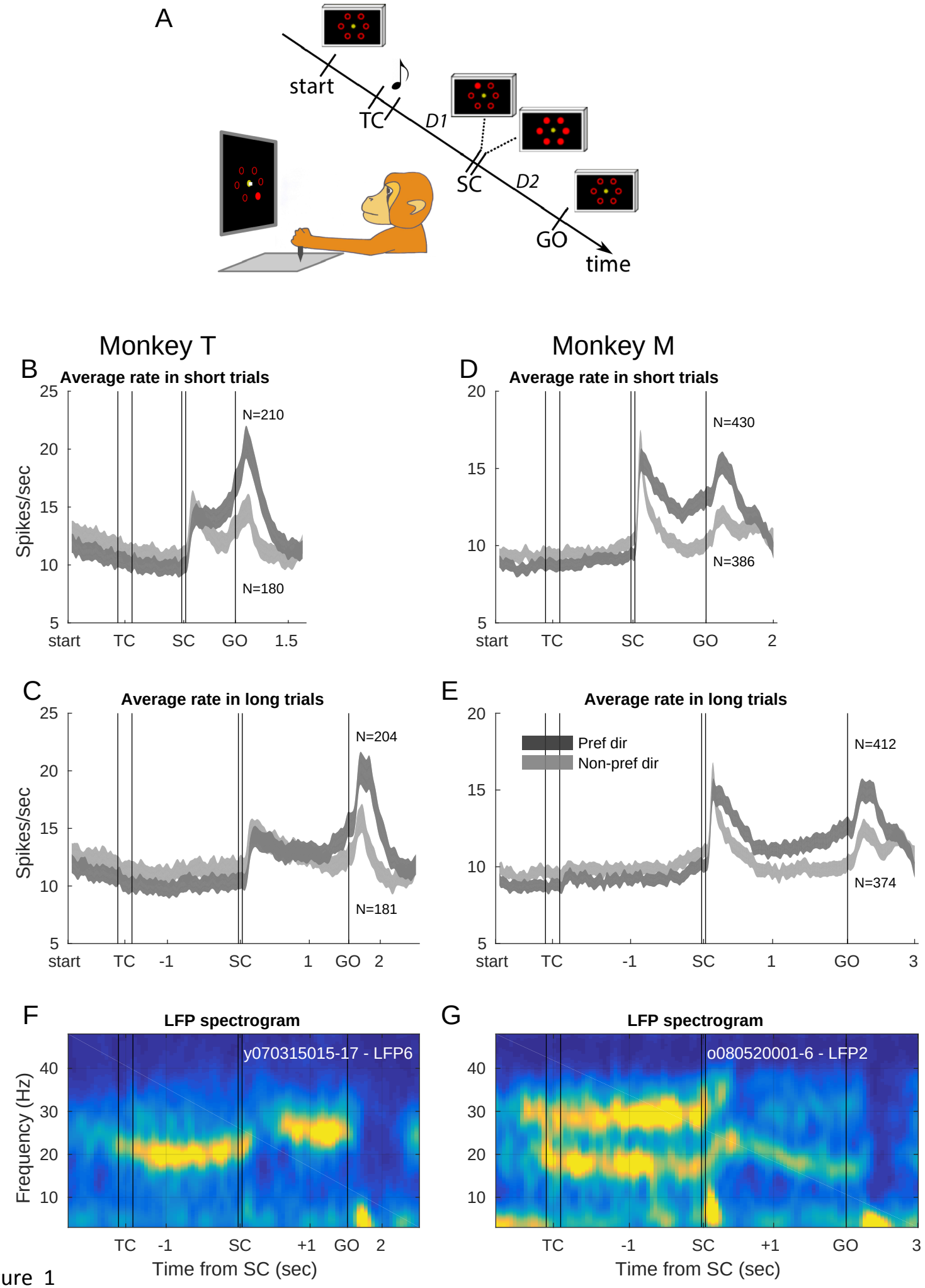
A
start
TC
D1
SC
D2
GO
time
Monkey T
B
Average rate in short trials
N=210
N=180
Spikes/sec
start
TC
SC
GO
1.5
Monkey M
D
Average rate in short trials
N=430
N=386
start
TC
SC
GO
2
C
Average rate in long trials
N=204
N=181
Spikes/sec
start
TC
-1
SC
1
GO
2
E
Average rate in long trials
Pref dir
Non-pref dir
N=412
N=374
start
TC
-1
SC
1
GO
3
F
LFP spectrogram
y070315015-17 - LFP6
Frequency (Hz)
TC
-1
SC
+1
GO
2
Time from SC (sec)
G
LFP spectrogram
o080520001-6 - LFP2
TC
-1
SC
+1
GO
3
Time from SC (sec)

Figure 1

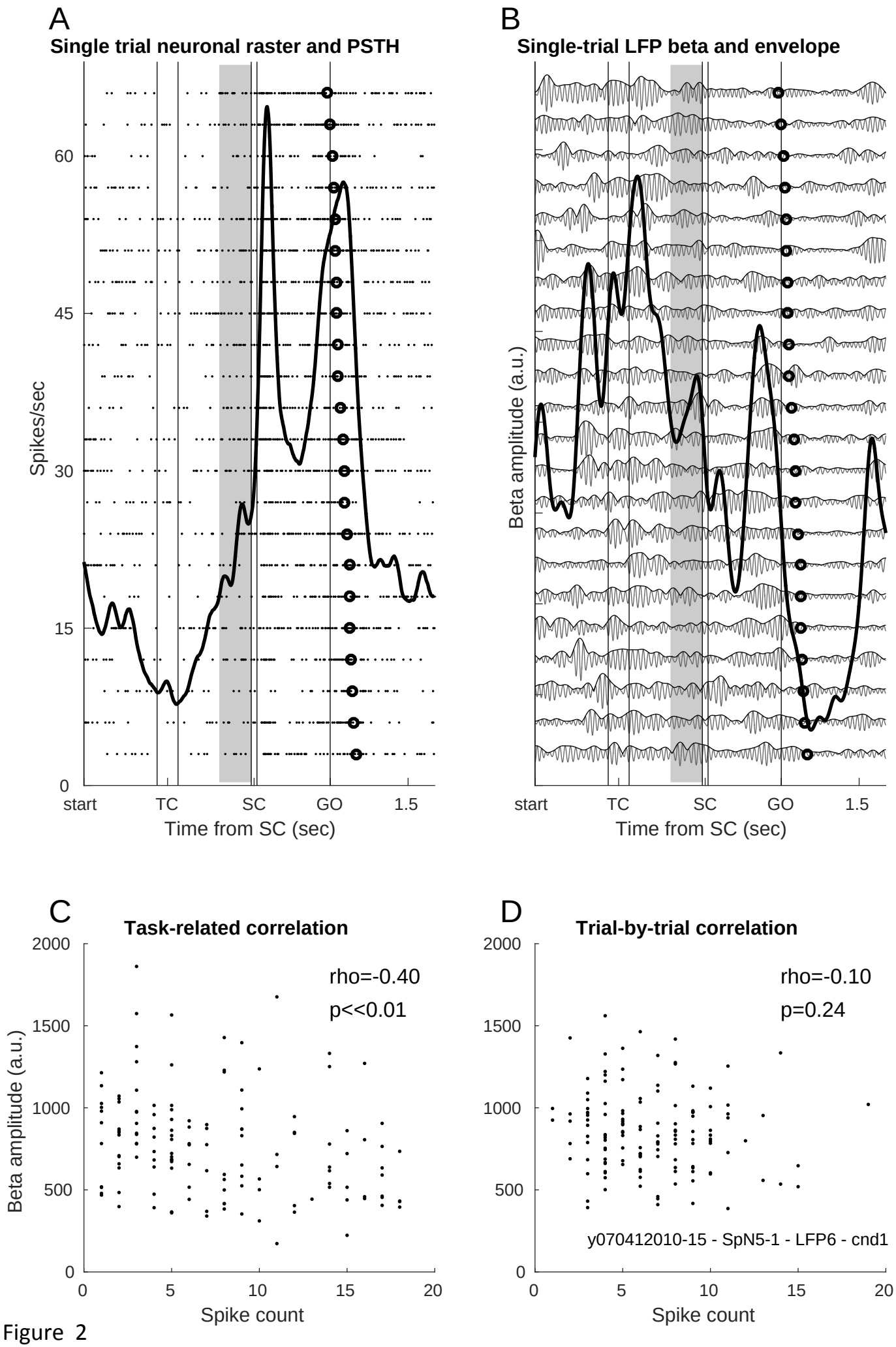
A
Single trial neuronal raster and PSTH
Spikes/sec
0
15
30
45
60
start
TC
SC
GO
1.5
Time from SC (sec)
B
Single-trial LFP beta and envelope
Beta amplitude (a.u.)
start
TC
SC
GO
1.5
Time from SC (sec)
C
Task-related correlation
rho=-0.40
p<<0.01
Beta amplitude (a.u.)
0
500
1000
1500
2000
0
5
10
15
20
Spike count
D
Trial-by-trial correlation
rho=-0.10
p=0.24
y070412010-15 - SpN5-1 - LFP6 - cnd1
0
500
1000
1500
2000
0
5
10
15
20
Spike count

Figure 2

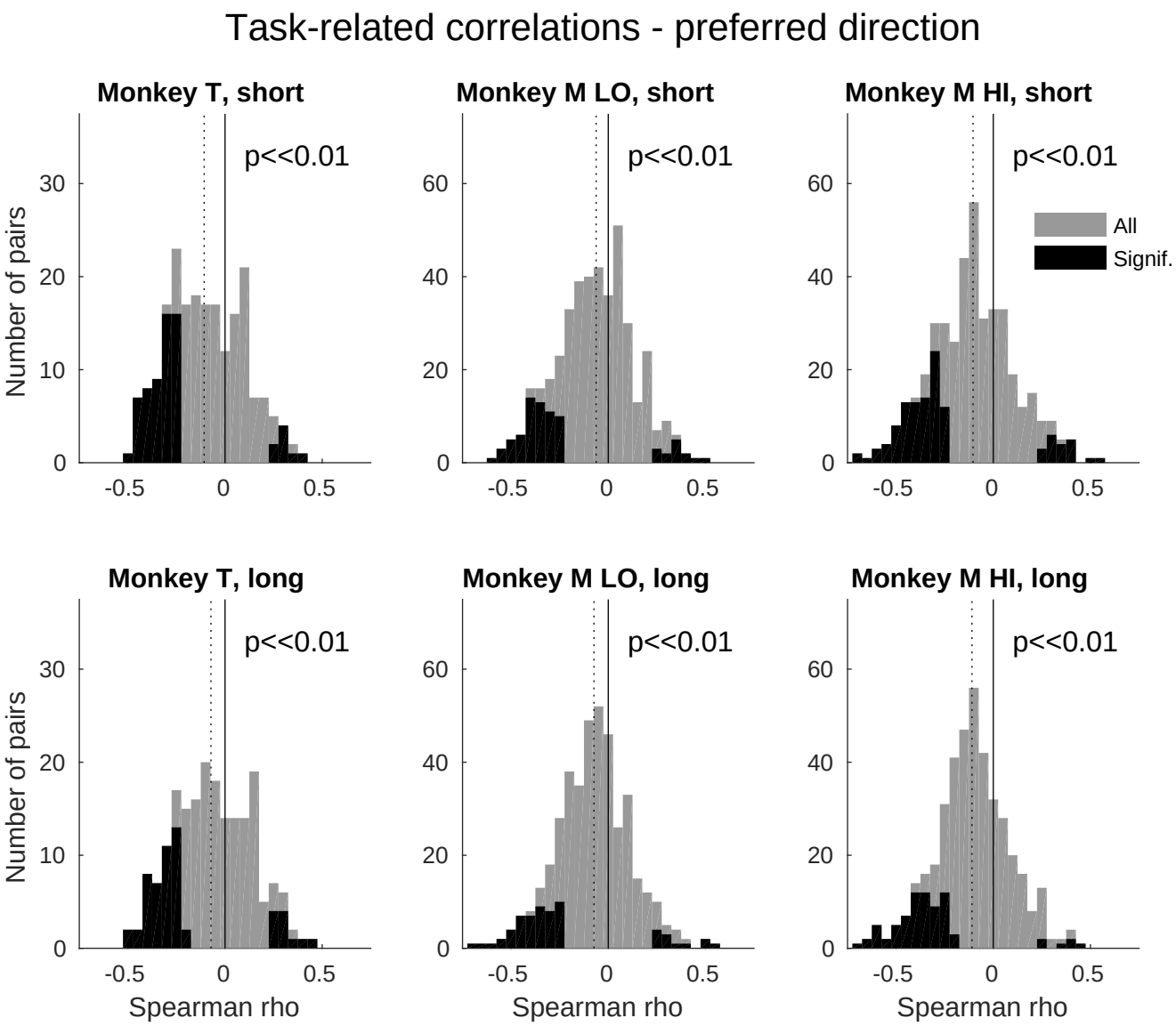
Task-related correlations - preferred direction
Monkey T, short
Monkey M LO, short
Monkey M HI, short
Monkey T, long
Monkey M LO, long
Monkey M HI, long
p<<0.01
All
Signif.
Number of pairs
Spearman rho

Figure 3

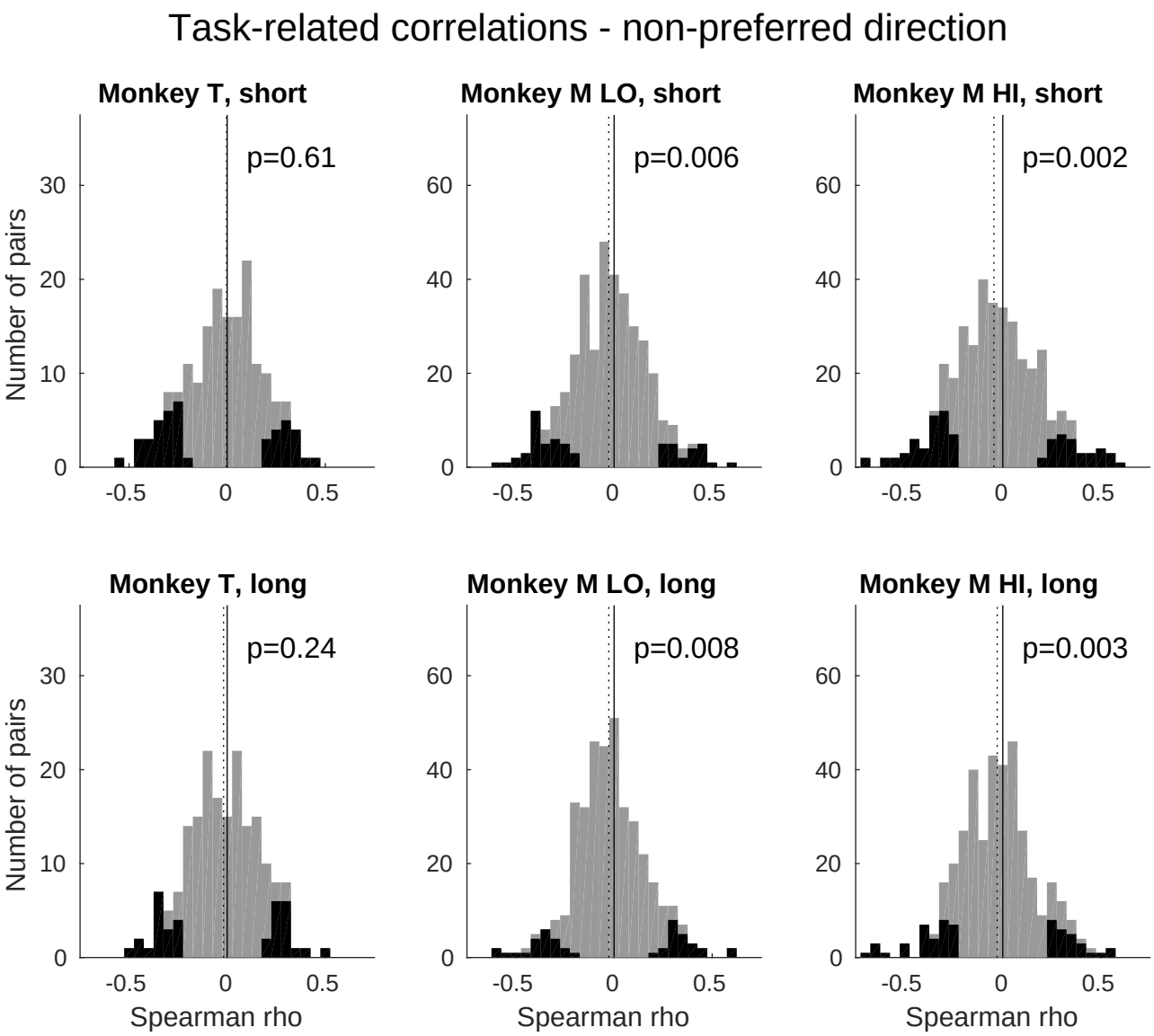
Task-related correlations - non-preferred direction
Monkey T, short
p=0.61
Monkey M LO, short
p=0.006
Monkey M HI, short
p=0.002
Monkey T, long
p=0.24
Monkey M LO, long
p=0.008
Monkey M HI, long
p=0.003
Number of pairs
Spearman rho

Figure 4

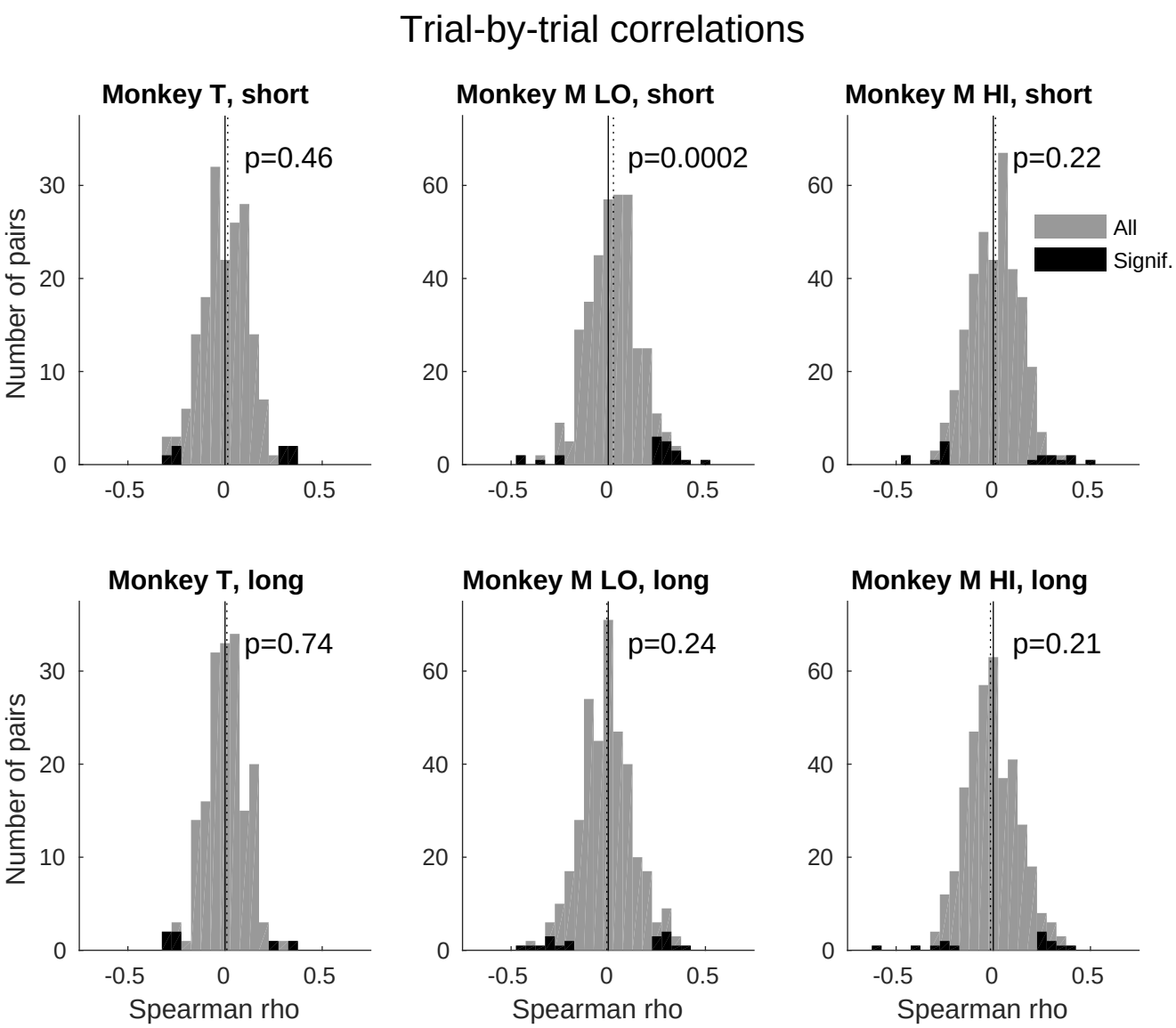
Trial-by-trial correlations
Monkey T, short
p=0.46
Monkey M LO, short
p=0.0002
Monkey M HI, short
p=0.22
All
Signif.
Monkey T, long
p=0.74
Monkey M LO, long
p=0.24
Monkey M HI, long
p=0.21
Number of pairs
Spearman rho

Figure 5

Table 1

Analysis	Data selection	Monkey T @ 22Hz		Monkey M LO @ 19Hz		Monkey M HI @ 32Hz	
		Significant	Negative Corr.	Significant	Negative Corr.	Significant	Negative Corr.
Task-related correlation All available windows	Short delay Preferred direction	104/210 (50%)	84/104 (81%)	177/430 (41%)	133/177 (75%)	205/430 (48%)	174/205 (85%)
	Short delay Non-preferred direction	69/180 (38%)	33/69 (48%)	139/386 (36%)	83/139 (60%)	167/386 (43%)	104/167 (62%)
	Long delay Preferred direction	88/204 (43%)	72/88 (82%)	175/412 (42%)	140/175 (80%)	202/412 (49%)	165/202 (82%)
	Long delay Non-preferred direction	74/181 (41%)	36/74 (49%)	138/374 (37%)	87/138 (63%)	153/374 (41%)	97/153 (63%)
Task-related correlation same # of windows as # of trials	Short delay Preferred direction	65/209 (31%)	57/65 (88%)	77/423 (18%)	63/77 (82%)	114/423 (27%)	94/114 (82%)
	Short delay Non-preferred direction	44/177 (25%)	26/44 (59%)	61/384 (16%)	38/61 (62%)	84/384 (22%)	49/84 (58%)
	Long delay Preferred direction	56/199 (28%)	45/56 (80%)	62/413 (15%)	50/62 (81%)	76/413 (18%)	70/76 (92%)
	Long delay Non-preferred direction	35/186 (19%)	18/35 (51%)	45/376 (12%)	22/45 (49%)	60/376 (16%)	34/60 (57%)
Trial-by-trial correlation	Short delay	7/178 (3.9%)	3/7	21/374 (5.6%)	5/21	17/374 (4.5%)	8/17
	Long delay	6/176 (3.4%)	4/6	18/378 (4.8%)	9/18	14/378 (3.7%)	6/14